

# MaTrEx AM: a new hybrid additive manufacturing process to selectively control mechanical properties

Amirpasha Moetazedian<sup>\*a</sup>, James Allum<sup>\*a</sup>, Andrew Gleadall<sup>a\*\*</sup>, Elisa Mele<sup>b</sup> and Vadim V Silberschmidt<sup>a</sup>

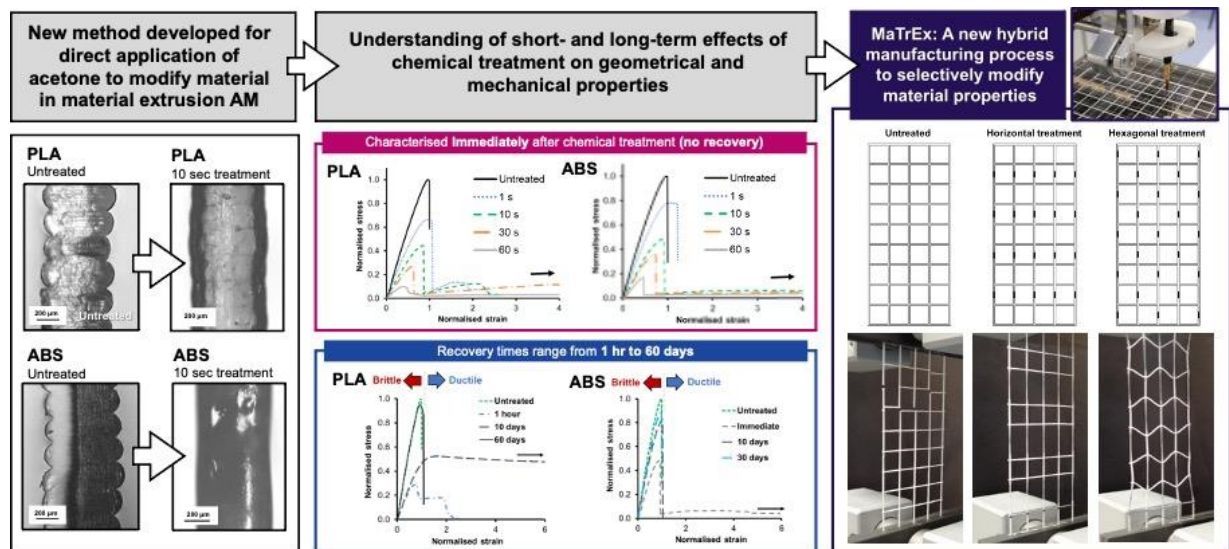
<sup>a</sup> Wolfson School of Mechanical, Electrical and Manufacturing Engineering, Loughborough University, Loughborough, LE11 3TU, UK

<sup>b</sup> Department of Materials, Loughborough University, Loughborough, LE11 3TU, UK

<sup>\*</sup>AM and JA contributed equally to this work.

<sup>\*\*</sup>Corresponding author - Email: [A.Gleadall@lboro.ac.uk](mailto:A.Gleadall@lboro.ac.uk)

## Graphical abstract



## Abstract

This study is the first to demonstrate how mechanical and geometrical properties of polylactide (PLA) and acrylonitrile butadiene styrene (ABS) additively manufactured with material extrusion can be selectively tailored using a newly devised treatment method of chemical immersion in acetone. This combination of manufacturing and chemical treatment results in a hybrid process capable of modifying mechanical behaviour in a predictable and time-controlled manner. Key new understanding is generated by analysing short-term effects (tested immediately after immersion) on mechanical and geometrical properties of printed specimens, with different immersion times (1 to 60 seconds) causing significant increases in strain-at-

fracture - up to 25- and 16-fold for PLA and ABS, respectively. In the long-term mechanical properties were found to recover by up to 90% of those for untreated specimens in ABS within 3 hours, while PLA properties recovered after 60 days. Importantly, while mechanical properties in both PLA and ABS recovered, the geometrical changes were retained. Annealing allowed the recovery time to be shortened: PLA specimens achieved full recovery within 24 hours. Chemical immersion provides significant advantages over widely used vapour-based treatment methods, since it allows selective application to achieve and localised changes of mechanical and geometrical properties. Applications of this new hybrid process, called Material Treatment Extrusion Additive Manufacturing (MaTrEx AM), are presented, including the capability to add new functionality (dramatically increased plasticity) to material structures manufactured with PLA and ABS. The implementation of MaTrEx AM as a hybrid manufacturing system is demonstrated. MatrEX AM enabled selective, localised modification of mechanical properties to increase toughness and redirect strain into selected regions of a mesh material.

**Keywords:**

Additive manufacturing; Chemical treatment; Mechanical recovery; Mechanical properties; Hybrid manufacturing

## **Nomenclature**

ABS – acrylonitrile butadiene styrene  
AM – additive manufacturing  
DSC – differential scanning calorimetry  
EFWs – extruded filaments widths  
 $I_T$  – immersion time in acetone  
MaTrEx AM – Material Treatment Extrusion Additive Manufacturing  
MEAM – material extrusion additive manufacturing  
PLA – polylactide  
 $R_T$  – recovery time after exposure to acetone  
 $T_{cc}$  – cold crystallisation temperature  
 $T_g$  – glass transition temperature  
 $T_m$  – melting temperature

## **1 Introduction**

Material Extrusion Additive Manufacturing (MEAM) is a method of 3D printing which has seen significant technological development in recent years. Among its benefits is the ability to rapidly manufacture bespoke parts with complex geometries, which are often prohibitively costly or time consuming to achieve by traditional subtractive manufacturing methods. This technology

has attracted significant research interest and investment from high-value industries including biomedical [1,2] and aerospace sectors [3,4].

MEAM operates by the extrusion of a molten polymer filament, which is deposited via a heated nozzle onto a print platform, where it rapidly solidifies. Typically, the nozzle moves in the X and Y planes (parallel to the print platform) to generate layers of parts sequentially. The lowering of the print platform in the Z direction at completion of each layer enables deposition of subsequent layers, leading to a layer-wise production. The completed part is the physical embodiment of the toolpath and appears as comprised of stacked micro-slices. Such a layer-wise methodology gives rise to the biggest limitation in MEAM - mechanical anisotropy, particularly weakness in Z direction [5–9].

Historically, this anisotropy has been attributed to deficiencies in interlayer bonding [10–18]. However, recent studies by the authors challenged the theory of bond deficiency based on microscale characterisation methods [19–22], demonstrating that bulk-strength interlayer properties can be achieved in MEAM for a range of printing conditions. Also, it was consistently evidenced that the true cause of interlayer weakness is geometrical, with naturally occurring filament-scale grooves causing stress concentration and reducing a load-bearing area by narrowing the bond region [19–21].

Chemical treatment of 3D-printed polymers was historically used for aesthetic reasons to improve the so-called ‘poor surface finish’ resulting naturally in MEAM due to grooves on the surface. That this surface finish could be detrimental to mechanical properties, was the key justification for the research in this study into the effect of chemical treatment on mechanical properties. In general, there are two main types of chemical treatment methods, and both are applicable for acetone: (i) application of vapour and (ii) immersion in solution. The former can be used hot or cold and is the most commonly used technique for acrylonitrile butadiene styrene (ABS) [23–27]. Acetone vapours are believed to react with outer layers of ABS components, weakening the surface bonds, and increasing mobility of chains to a more stable condition [23]. The result of such a treatment is characterised by a smooth and polished surface commonly referring to as ‘re-melting’ of the polymer. Most studies focused on the surface finish of 3D-printed parts in terms of surface roughness. It is considered that methods employing hot vapour and immersion methods are difficult to control resulting in non-uniform smoothing. Also, the effects of smoothing on mechanical performance of 3D-printed polymers is not understood. This study aims to address this lack of knowledge. Most studies only considered the immediate (short-term) effect of acetone on 3D-printed polymers, while here we investigate important changes in the long-term (up to 60 days). Importantly, vapour-

smoothing is often considered only to be applicable for some polymers (including ABS) but not polylactide (PLA), which has a range of applications including high-value biomedical. To date, there are only a small number of studies which have considered the effects of chemical treatment on 3D-printed PLA [28–30]. However, these studies did not consider the interlayer mechanical performance. Furthermore, these studies did not analyse the evolution of mechanical and geometrical properties over time. The application of this findings may be limited due to the use of a toxic solvent (chloroform).

Herein, for the first time, both the short- and long-term effects of a solvent (acetone in this case) on 3D-printed ABS and PLA are considered. A new hybrid process combining direct application of acetone and AM (MaTrEx AM) was introduced. The knowledge developed in the first part of this study, focused on short-term effects of chemical treatment, informed the selection of an appropriate exposure time to analyse the long-term effect of acetone with respect to the recovery of mechanical properties. The applicability of the obtained results is discussed in terms of providing new opportunities in the MEAM area by applying the novel methods and understanding developed to selectively modify the properties of additively manufactured components in a controlled and predictable manner and thus enhance the mechanical and manufacturing capabilities of MEAM.

## **2 Materials and methods**

### **2.1 Materials**

Two most commonly used 3D-printable polymer materials were used in their pure form (no colourants or other additives), to manufacture specimens: (i) polylactide (3DXTECH® branded NatureWorks® polylactide 4043D, Sigma Aldrich) and (ii) acrylonitrile butadiene styrene (3DXMAX® branded NatureWorks®, Sigma Aldrich).

### **2.2 Additive manufacturing process**

A RepRap X400 3D-printing system with 0.4 mm nozzle was used to produce specimens. Custom GCode was generated using in-house-developed software (“FullControl GCode designer”, available from [www.fullcontrolgcode.com](http://www.fullcontrolgcode.com)) with set printing parameters (see Table 1) for ABS and PLA to produce a four-sided hollow box with wall dimensions of 45 mm x 45 mm comprising single-filament walls (0.5 mm thick) (Figure 1ai). By controlling the extrusion volume directly in the GCode, the extruded filament widths varied from 0.75 (shoulder region) to 0.5 mm (gauge regions) to achieve dogbone tensile-testing specimens [19].

The single-filament design was used to allow precise mechanical and geometrical characterisations of specimens at the smallest possible scale – the bond between individual

extruded filaments. The current design and overall dimensions are adapted from the ASTM D1708 microtensile specimen [31] and have been validated in several previous studies [20,32].

**Table 1** Printing parameters used to produce ABS and PLA specimens with RepRap x400 system.

| Printing parameters                       | ABS  | PLA  |
|---|------|------|
| Extrusion temperature (°C)                | 250  | 210  |
| Print platform temperature (°C)           | 100  | 60   |
| Printing speed (mm.min <sup>-1</sup> )    | 1000 | 1000 |
| Extruded layer height (mm)                | 0.2  | 0.2  |
| Extruded filament width within gauge (mm) | 0.5  | 0.5  |

In this study, the main focus is on the effect of chemical treatment on grooves, which naturally occur in the interlayer bond region between extruded filaments deposited during the MEAM process. Thereby, the weakest mechanical orientation (i.e. normal to the interface between layers) was chosen as it is considered the most critical aspect, limiting the mechanical application of MEAM.

For characterisation of the specimens, each printed box was cut into 5 mm wide and 45 mm tall specimens (Figure 1a) according to the following steps [20]:

1. The box corners were cut using a specially designed tool with a razor blade to yield four walls.
2. Each wall was cut with another specially designed tool, comprising an array of seven razor blades with 5 mm spacing.

A 12-tonne hydraulic press was used for a controlled and even cutting process by compressing the blades into walls to produce twenty-four specimens from each box. No edge effect was observed in the cutting process: the mechanical properties of specimens with different width (5 and 15 mm) were compared with those of injection-moulded polymer and no significant difference was found as shown by authors in another study [19]. Specimens and materials were stored in sealed bags with silica desiccant in laboratory conditions (20°C and 50% relative humidity (RH)).

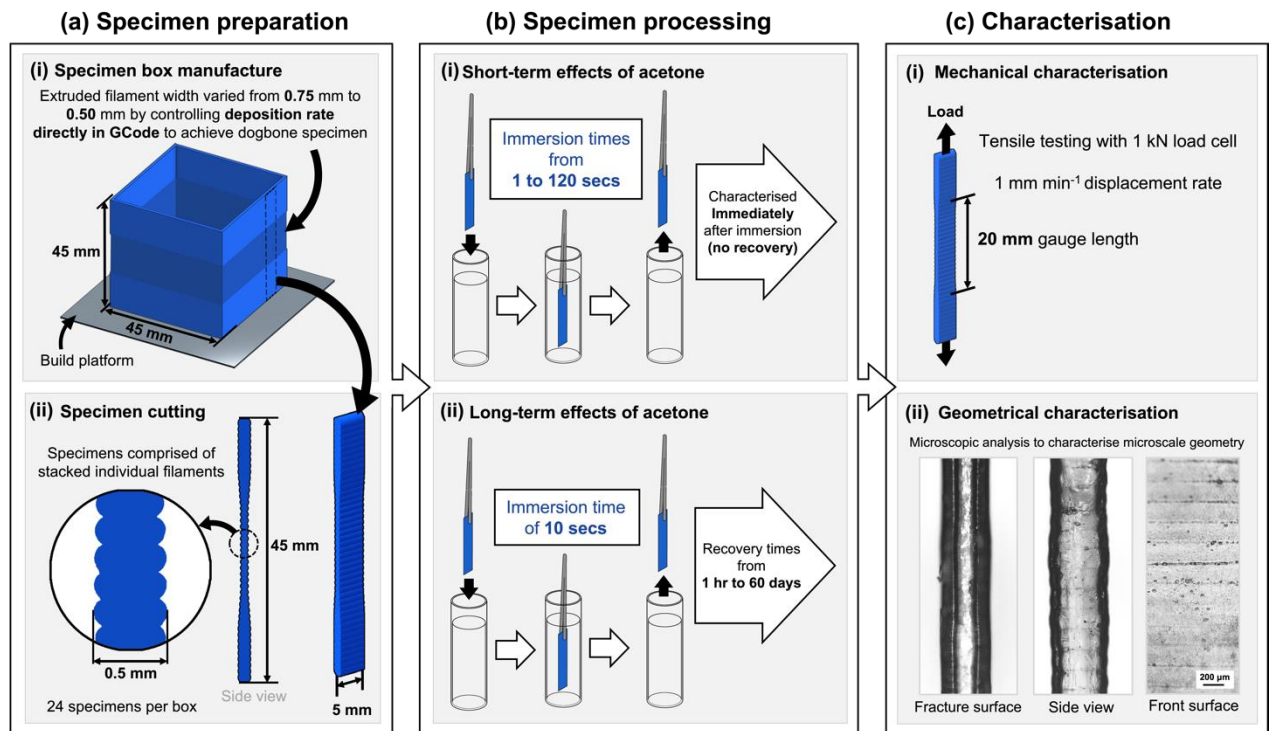


**Figure 1** Schematic of the overall layout of this study. (a) Specimens preparation involves manufacturing of single-filament box (i) and cutting each box into 5 mm wide and 45 mm tall specimens (ii). (b) Specimens were directly exposed via immersion in acetone for periods from 1 to 120 s (i) to evaluate short-term effects of acetone and drying specimens immersed for 10 s for 1 hour up to 60 days (ii) to evaluate long-term effects. (c) For both short- and long-term effects, mechanical and geometrical characterisations were carried out.

### 2.3 Chemical treatment

Both ABS and PLA specimens ( $n=4$  for each material) were directly exposed via immersion in 30 ml of pure acetone for 1, 10, 30, 60 and 120 s (referred to as *immersion time* ( $I_T$ )). After each immersion period, specimens were removed from the solution and excess acetone was removed by gentle agitation in air. The specimens were left in laboratory conditions (20°C and 50 RH) for 1 minute, after which the short-term effect of acetone exposure on both ABS and PLA was considered immediately (without further recovery time) (Figure 1b) by means of mechanical (Figure 1ci) and geometrical characterisation (Figure 1cii).

Based on data from preliminary tests, a 10 s immersion time was selected for assessment of long-term effects of acetone on polymers. Following this, treated specimens were left to dry in laboratory conditions (20°C and 50% RH) for 1 hour, 3 hours, 1 day, 5 days, 10 days, 30 days and 60 days (referred to as *recovery time* ( $R_T$ )) prior to mechanical (Figure 1ci) and geometrical characterisation (i.e. monitoring the changes in the texture and/ or filament-scale grooves) (Figure 1cii). In addition, a hybrid manufacturing system which directly applies acetone in-situ during the manufacturing process was developed and is discussed in Section 4.

## 2.4 Mass tracking

The evolution of acetone absorption and its evaporation for both ABS and PLA (n=3 for each material) was studied by weighing the specimens before and after chemical treatment until the mass had stabilised. Mean values were calculated from three replicates and the data were normalised with the initial mass.

## 2.5 Tensile testing

ABS and PLA specimens (n=4 for each material) were tested in uniaxial tension (under laboratory conditions) using a universal testing machine (Instron 5944) at a constant displacement rate of 1.0 mm min<sup>-1</sup> (8.3 x 10<sup>-4</sup> s<sup>-1</sup> strain rate) using a 1 kN load cell (Figure 1c). A Zeiss Primotech optical microscope with 5x magnification was utilised together with ImageJ software to measure a pre-fracture cross-sectional area using the methodology described previously [20]. ImageJ software was also employed to measure the mean bond angles for all specimen types from 10 measurements. The tensile modulus was calculated from the linear region of the stress-strain curves. The toughness value (ability to absorb energy during plastic deformation until failure) was assessed based on the area underneath a stress-strain curve.

## 2.6 Optical microscopy

The fracture surface, front surface (i.e. the view of the box wall) and cross-sectional side-views of each specimen, as shown in Figure 1c, were examined using a Zeiss Primotech optical microscope at various magnifications.

## 2.7 Differential scanning calorimetry

Thermal properties of specimens (n=3) were examined using a TQ2000 (TA, instrument, USA) Differential Scanning Calorimetry (DSC) system. Approximately 10 mg (from the gauge region) were cut and loaded onto the aluminium pans (weight of 6-10 mg). Thermal analysis was carried out using heating cycles from 20 to 200°C at a ramping rate of 10°C.min<sup>-1</sup> and a nitrogen flow rate of 50 ml.min<sup>-1</sup>. The obtained thermograms were analysed using TA Universal software to determine glass transition temperature (T<sub>g</sub>), melting temperature (T<sub>m</sub>) and cold crystallisation temperature (T<sub>cc</sub>). The average degree of crystallinity (X<sub>c</sub> %) was calculated from two measurements for specimens:

$$X_c = \frac{f_m - f_{cc}}{f_m} \times 100 \quad (3)$$

where  $f_m$ ,  $f_{cc}$  and  $f_m^0$  are melting enthalpy (J.g<sup>-1</sup>), cold crystallisation enthalpy (J.g<sup>-1</sup>) and enthalpy of fusion for 100% crystalline PLA, which is 93.1 J.g<sup>-1</sup> [19,33].

## **3 Results and discussion**

### **3.1 Development of direct chemical treatment method**

While vapour treatment with acetone has been shown as a viable post-processing solution, particularly for aesthetic purposes, it fails to provide the selective treatment desired to support a hybrid manufacturing process [23]. Our hypothesis was that by improved application of chemical treatment with better understanding of mechanical and time-dependant influences it would be possible to develop a hybrid manufacturing process. To achieve this, it was necessary to understand the effect of acetone on mechanical properties. Preliminary tests ruled out the use of vapour treatment as it did not enable selective or complete exposure, as outlined in supplementary data. Therefore, direct application of acetone on specimens was investigated as this approach could translate into a selective treatment method.

To undertake mechanical and material evaluation, the direct application of acetone was achieved by complete immersion of specimens formed of individual extruded filaments (Figure 2a). This method was evaluated and refined prior to the main study (Figure 2 (b) to (d)) to ensure applicability for time dependant studies and to develop a protocol (as outlined in Section 2.3). To assess modifications produced by this process, the short- and long-term effects of direct application of acetone on mechanical and geometrical characteristics of PLA and ABS specimens were analysed.

The method of direct application of acetone via immersion informed the development of a new hybrid manufacturing process by translating the direct exposure of acetone via immersion to a droplet-scaled selective exposure process that achieved localised material property modifications, presented in Section 4.

### **3.2 Short-term effects of acetone**

This section summarises the results of the immediate testing of specimens after direct application of acetone to develop an understanding of the effects of this solvent on various physical (Section 3.2.1) and mechanical (3.2.2) properties, and to identify the relationships between material properties and geometrical variation (3.2.3) of 3D-printed polymers.

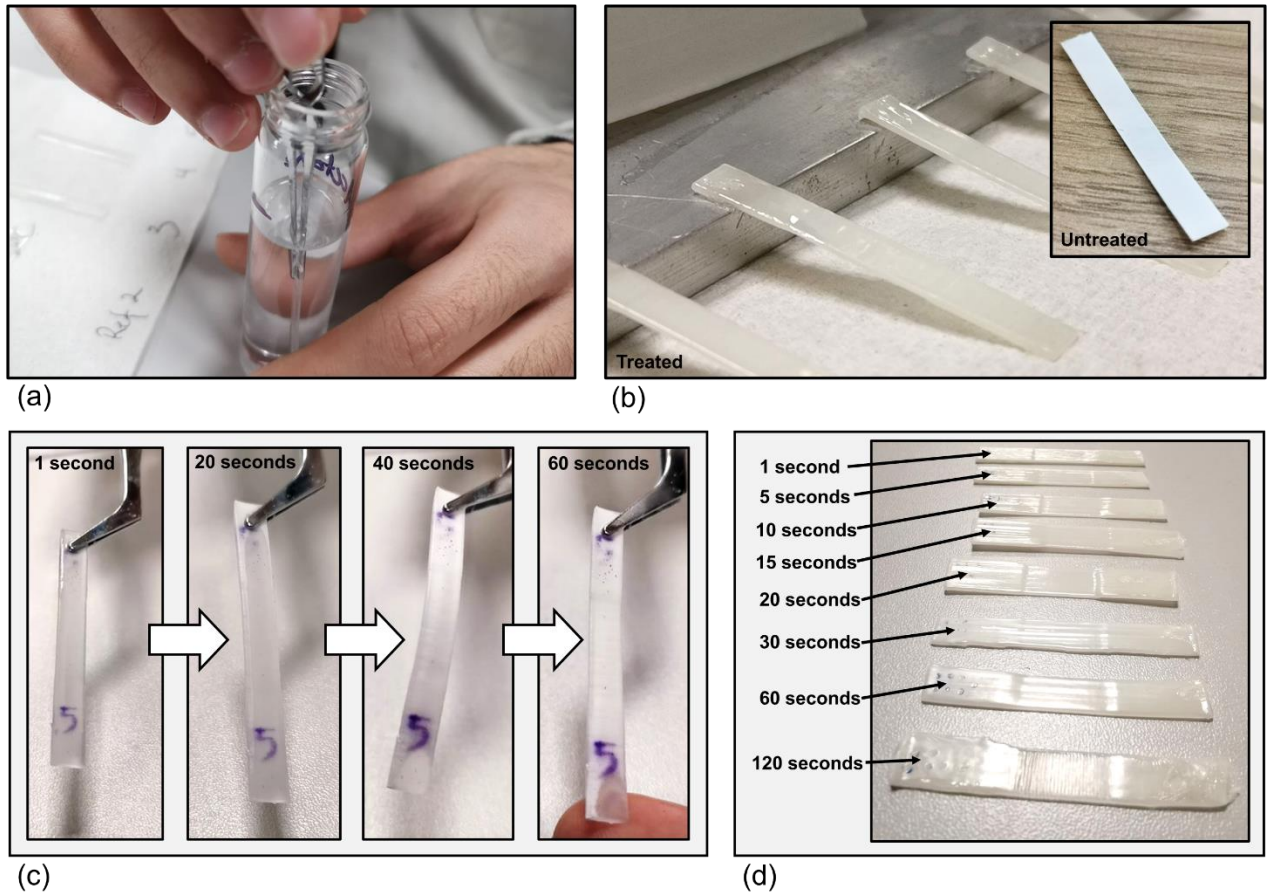


**Figure 2** Chemical treatment of ABS and PLA by immersion (a) showed visible changes to ABS (b) compared to the untreated specimen (inset in (b)). PLA evolved at different time intervals after immersion (c). (d) The difference in levels of smoothing of both PLA and ABS appeared to be dependent on the immersion time (shown here for ABS).

### 3.2.1 Mass tracking and geometrical changes

The first step was to monitor the evolution of the acetone absorption and its evaporation for both 3D-printed PLA and ABS up to 20 days. For visualisation of the data, only results for the first hour are presented since the mass of both PLA and ABS specimens stabilised after that time point. Furthermore, the mass data were normalised by the initial specimen mass (i.e. prior to immersion) to allow direct comparison.

As demonstrated in Figure 3, the obtained results can be explained in terms of the similarities and differences for the two polymers. Both polymers absorbed acetone immediately, but to different extent. PLA absorbed a gradually greater normalised mass: 1.18, 1.18, 1.32 and 1.38 after 1, 10, 30 and 60 sec, respectively. Meanwhile, ABS absorbed less: 1.21, 1.06, 1.16, 1.18 after 1, 10, 30 and 60 sec, respectively. Also, monitoring the evaporation of acetone (after removal of the specimens from acetone) showed stabilisation of mass after just 5 mins for ABS (this mass plateau was retained up to the 20-day point), whereas PLA took 15 mins to reach the mass-stabilisation state. When considering the net mass after stabilisation, PLA

gain mass, while ABS lost mass (except for the 1 s immersion time), likely because ABS is soluble in acetone. Such results clearly demonstrated a difference in terms of the interaction of acetone with the two distinct polymer types. Also, acetone appeared to become entrapped within the PLA specimens, but this was not apparent in ABS (as discussed in Section 3.2.3). In side-view micrographs of all specimens (taken for qualitative analysis), the grooves naturally introduced in the MEAM became less apparent with the surface becoming incrementally smoother as immersion time was increased (Figure 3). Grooves were apparently removed after only 10 sec of immersion for ABS, while 60 sec was needed for the grooves in PLA specimens to be fully removed.

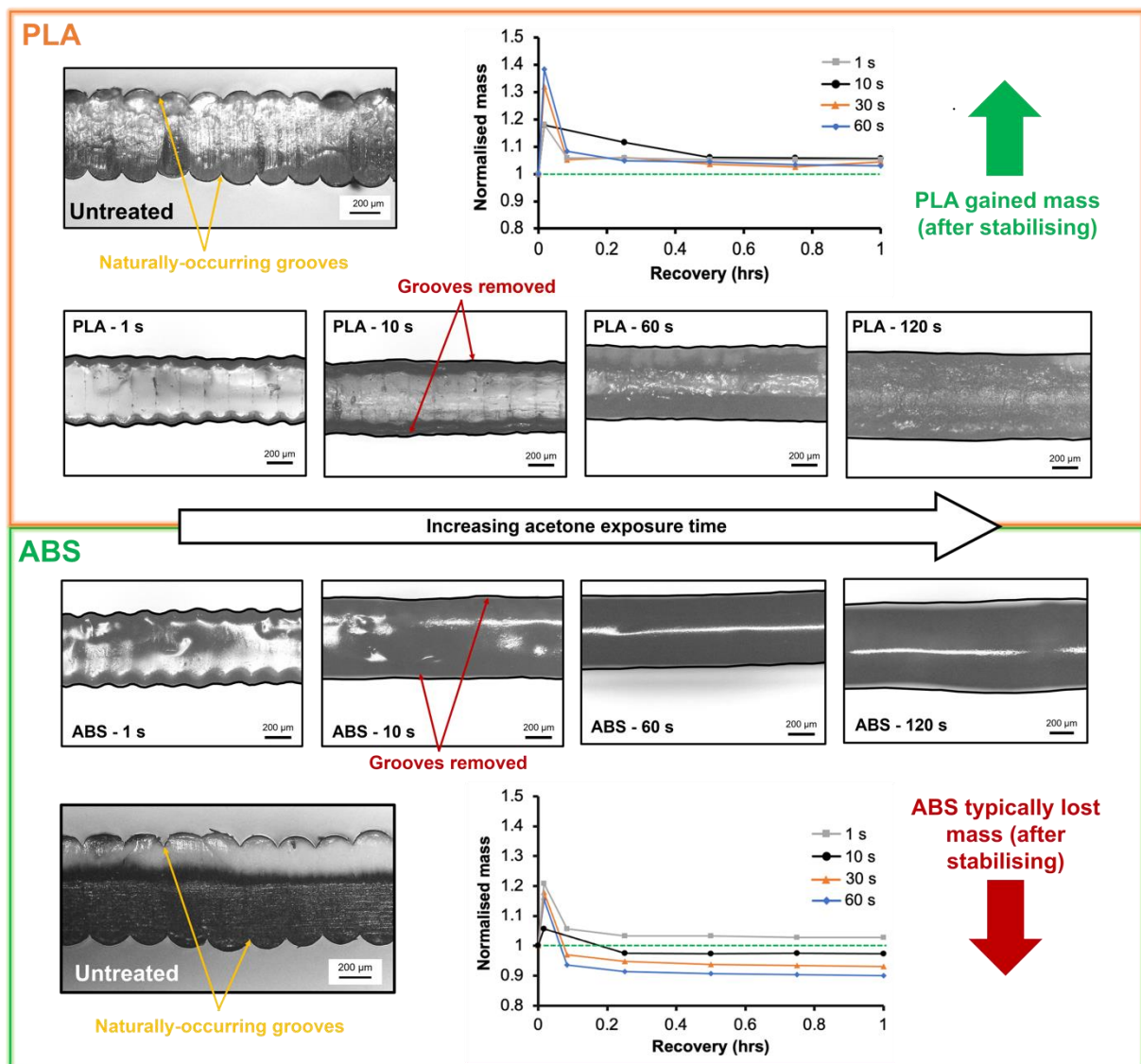


**Figure 3** Optical images show the extent of surface smoothing for PLA (top row) and ABS (bottom row) after dipping in acetone for various times. The magnitude of smoothing increased with the immersion time. Evolution of the normalised mass with recovery time for PLA and ABS after immersion in acetone for various times, demonstrated the mass gain for all immersion times in the former, whilst the latter showed mass loss (except for 1s). Black outlines have been annotated onto micrographs for clarity.

### 3.2.2 Mechanical properties

Immediately after exposure of the PLA and ABS specimens to acetone, their mechanical characterisation was undertaken (Figure 4). The obtained stress data were normalised by strength of the untreated bulk polymer (for PLA: 62.8 MPa and for ABS: 34.3 MPa). Apparently, both polymer types showed a reduction in stiffness as expected due to the plasticisation effect of acetone [34,35] (Figure 4), which significantly improved the strain-at-fracture, even for relatively brittle PLA. The acetone chemically interacted with both polymers and weakened the bonds [23] which appeared to reduce the maximum stress levels, values decreased by 29-87% for PLA and by 37-83% for ABS as immersion time increased compared to the untreated reference. Although these reductions are undesirable for load-bearing capabilities, properties do recover over time (Section 3.3). Also, the ability to control the onset of plasticity is valuable, particularly if localised control of properties is possible (Section 4). As anticipated, untreated specimens of PLA and ABS demonstrated a sudden brittle fracture due to the presence of micro-scale grooves (between 3D printed layers) which acted as stress concentrators as previously described [20]. In contrast, immediate changes in mechanical performance occurred when PLA and ABS were immersed for 1 s and 10 s, respectively. During tensile testing, these specimens produced a 'popping' noise, accompanied by a sudden reduction in their load-bearing capacity (indicated by dashed arrows in Figure 4) but without incurring complete failure of the specimens after considerable deformation (> 16-fold increase). On closer inspection, the popping phenomenon and associated incomplete fracture were caused by formation of a rubber-like skin on the exterior of the specimens during chemical treatment (visible in the inset micrograph images in Figure 4). This skin apparently acted as a protective layer by preventing the initial crack - a result of the fracture of the specimen's brittle core - from propagating outwards. The rubber-like deformation behaviour considerably improving the ductility.

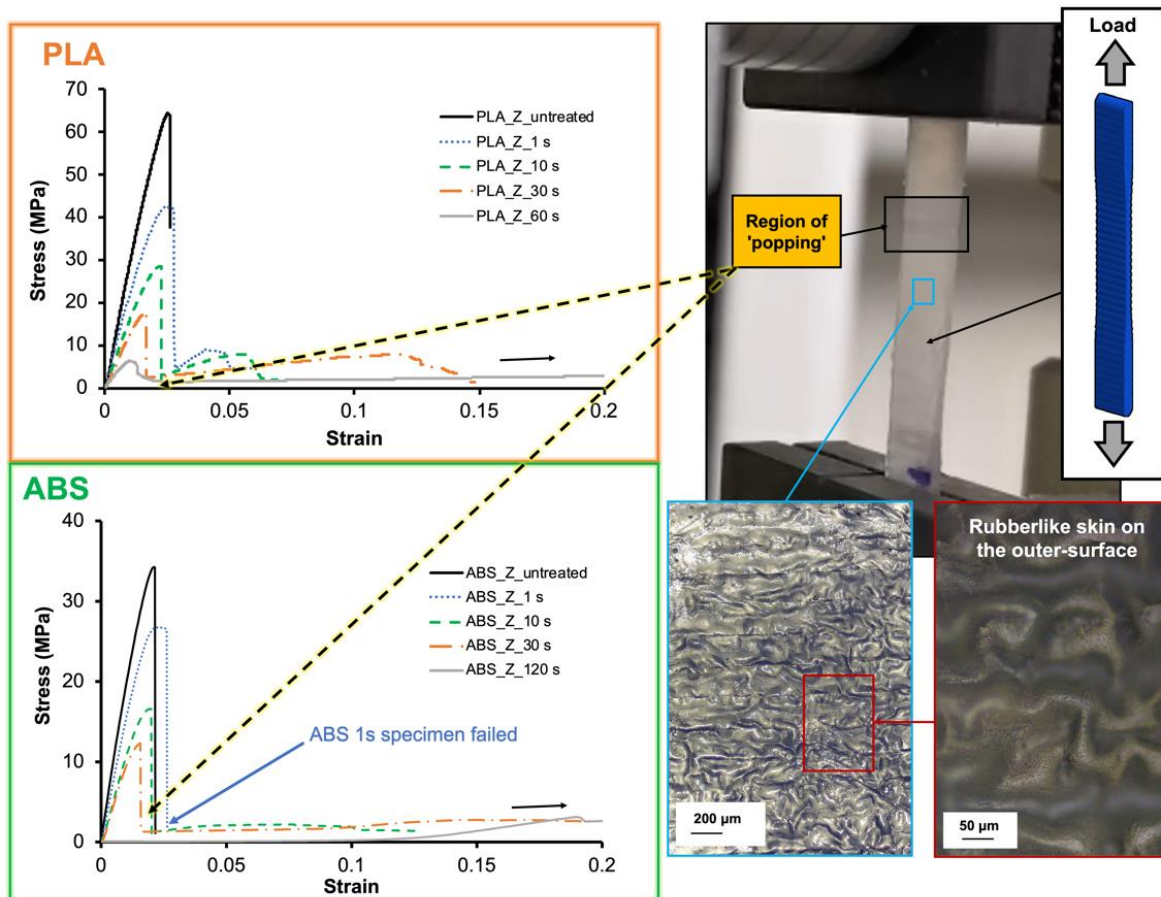


**Figure 4** Short-term effect of acetone immersion time on mechanical properties of PLA (top image) and ABS (bottom image). Acetone plasticised both polymers, lowering the stress levels whilst increasing ductility. The plasticity of polymer was associated with formation of a rubber-like skin on the outer-surface of both polymers, which prevented a brittle fracture of the core material.

From the stress-strain curves, average mechanical properties of each specimen type were calculated (Figure 5). They demonstrated a near linear declining trend for both ultimate tensile strength (UTS) and tensile modulus with similar magnitudes of reduction for specimens of both polymer types. Meanwhile, toughness (which is linked to both stress and strain levels) showed different trends. For PLA, toughness initially halved for immersion in acetone for up to 30 s, but, when specimens were treated for longer periods (e.g. 60 s), the toughness increased three-fold compared to the untreated specimens. Such a phenomenon could be explained by the changes in crystallinity of PLA discussed below. On the other hand, for fully amorphous ABS specimens, the toughness values were comparable or higher than those of the untreated polymer for immersion times of 10 s or more. This is not surprising given that ABS typically exhibits a considerable amount of plasticity (around 20%) prior to failure. Due to significant changes in mechanical properties of specimens in both polymers, the evolution of strain-at-fracture along with fracture analysis is considered in the next paragraph. Additionally, the thermal properties of PLA were measured in the next section to understand factors influencing the underlying mechanism for changes in properties.

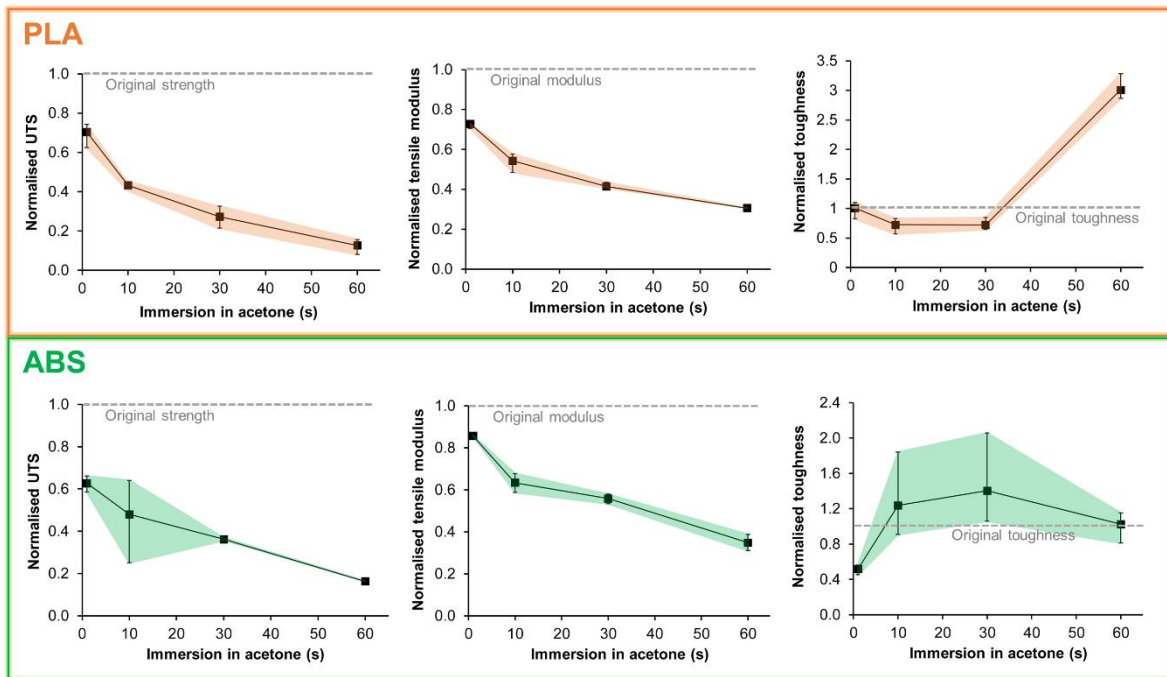


**Figure 5** Evolution of normalised UTS, tensile modulus and toughness for different acetone immersion time for PLA (top row) and ABS (bottom row). Shaded regions represent the range of data from four replicates.

As explained in the previous paragraphs, both polymers were affected by direct application of acetone in a similar manner but to different extents. The acetone plasticised PLA and ABS by increasing the strain-at-fracture 25- and 16-fold, respectively, compared to the untreated specimens (Figure 6). The fracture surfaces of each specimen type were examined (Figure 6) and untreated specimens showed flat and smooth surfaces, typical for a brittle fracture. Meanwhile, for specimens immersed in acetone for various times, a decrease in the brittle area was observed; quantification of this feature provided a better understanding with respect to mechanical properties. The width of the brittle area was measured in micrographs of fracture surfaces and these values were normalised by the width of the untreated specimen to calculate a parameter termed *brittle-ductile ratio*. As anticipated, this brittle-ductile ratio for each specimen type showed a trend of reduction as exposure time increased for both PLA and ABS specimens. An opposite trend was observed for strain-at-fracture, confirming an increase in plasticity of both polymer materials upon exposure to acetone. By comparing ABS and PLA, it was apparent that the increase in plasticity of ABS beyond 30 s resulted in complete disappearance of the brittle area (Figure 6). On the other hand, PLA demonstrated a small but measurable brittle area even after 30 s immersion in acetone. Such differences in the evolution of properties could be explained by the polymer chemistry and differences in the chemical interaction of the polymers with acetone. In particular, previous studies [34,35] for

non-additively manufactured PLA demonstrated that acetone acted as a plasticiser, at the same time inducing crystallisation for PLA. Based on these results, the analysis of the crystallisation was undertaken in the next section. The thermal analysis was only undertaken for PLA, since ABS is known as an amorphous polymer, crystallinity of the polymer cannot be measured.

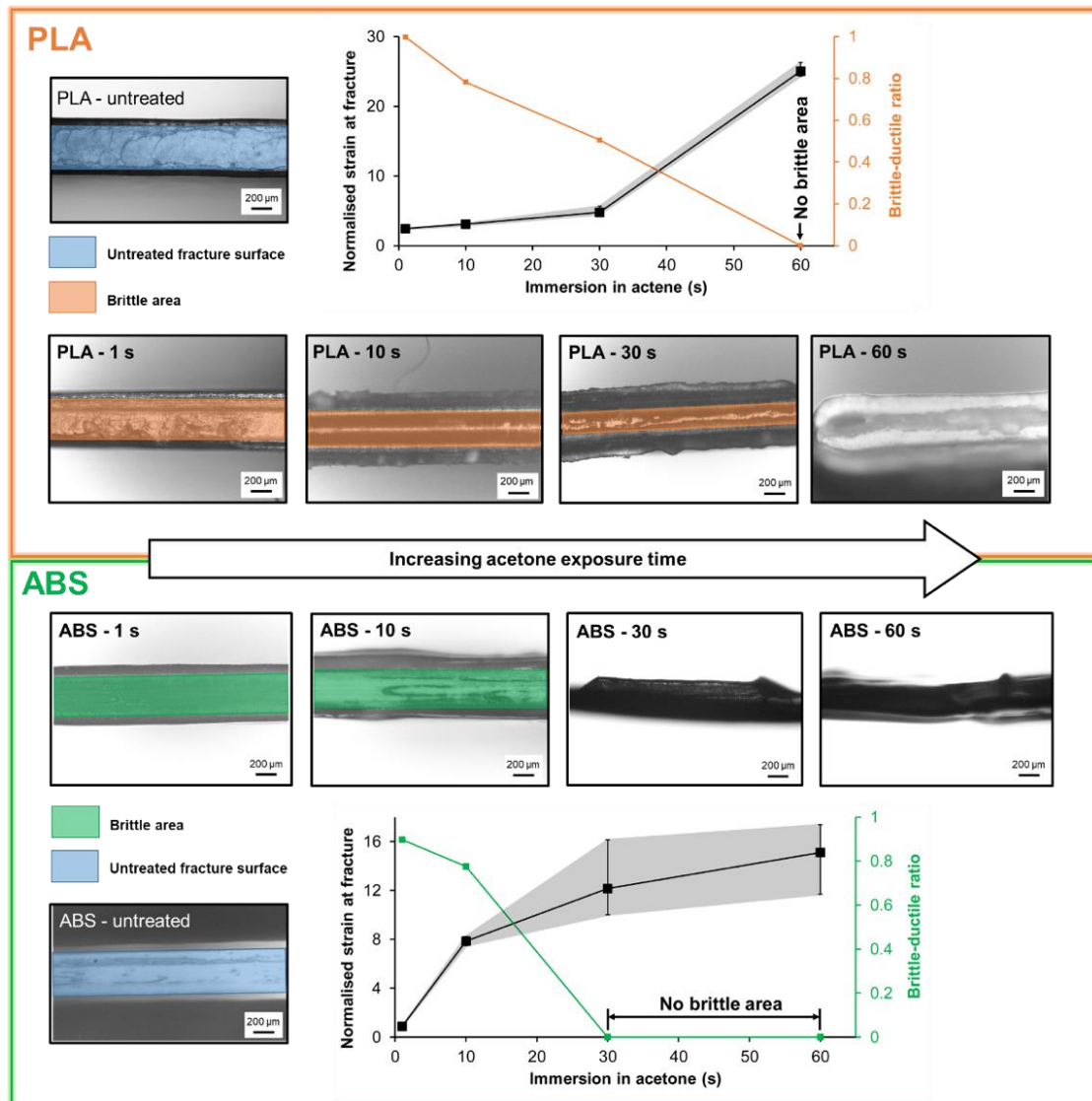


**Figure 6** Fracture surfaces of tested specimens for PLA (top row) and ABS (bottom row) immediately after exposure to acetone for various times. The graphs show the effect of immersion time on strain-at-fracture and brittle-ductile-ratio.

### 3.2.3 Thermal properties

The evolution of DSC thermograms and average crystallinity values for PLA immersed in acetone is demonstrated in Figure 7. The untreated PLA in this study had a crystallinity of 3.69% and  $T_g = 57.4^\circ\text{C}$  and  $T_m = 148.1^\circ\text{C}$ . Specimens immersed for just 1 s in acetone showed a secondary  $T_g$  around  $47.4^\circ\text{C}$ , lower than that of the untreated PLA. As immersion time increased,  $T_g$  was further reduced to  $39.1^\circ\text{C}$  (indication of plasticisation) and disappeared in

specimens immersed for longer than 30 s. A similar trend was identified for cold crystallisation temperature ( $T_{cc}$ ). The melting temperature ( $T_m$ ) also started to decrease from 148.1°C to 143.9°C after 120 s of immersion, whilst the intensity of exothermic peak for crystallisation increased. From DSC thermograms, the crystallinity of PLA specimens was calculated as 3.69%, 10.4%, 19.1%, 31.1%, 28.9% and 35.3% for the untreated specimens and immersion time of 1 s, 10 s, 30 s, 60 s and 120 s, respectively. Such results may be explained by supposing two main phases in the PLA specimens; (i) amorphous phase in the central (core) region without any contact/penetration by acetone; and (ii) crystalline phase induced by acetone, as supported by studies in literature [34,35]. The decrease in  $T_g$  derived from the plasticiser effect of acetone. Additionally, the reduction in  $T_{cc}$  and  $T_m$  with increasing time of exposure to acetone demonstrated that the crystallisation in the second phase could have induced the crystallisation of core region [34,35]. The DSC thermograms of specimens immersed for more than 30 s showed no trace of  $T_{cc}$  nor  $T_g$  in the temperature range analysed, confirming that acetone had reached their centre; this coincided with plateauing of crystallinity. These results clearly demonstrated that acetone had a dual effect by increasing both plasticisation and crystallinity of PLA more substantially than a typical annealing process.

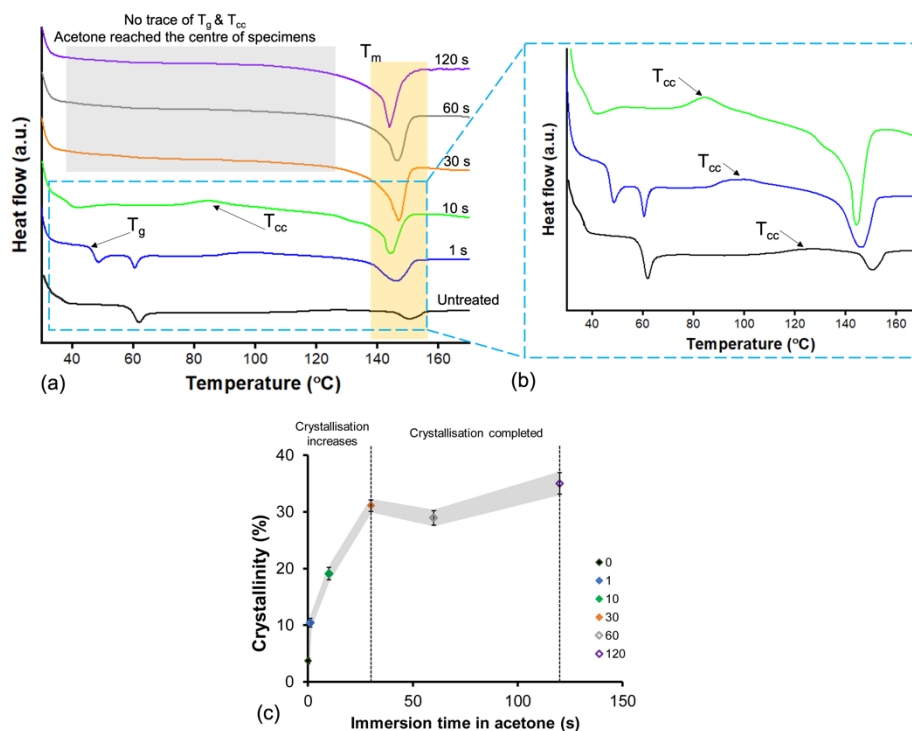


**Figure 7** (a) DSC curves for PLA after various times of immersion in acetone indicated the plasticisation of polymer due to the shift in  $T_g$ ,  $T_{cc}$  and  $T_m$  compared to the untreated specimen. (b) Zoomed-in insets for untreated, 1 s and 10 s specimens. The reduction in  $T_{cc}$  was related to induced crystallisation in the centre of specimens. The disappearance of  $T_{cc}$  after 30 s indicated that acetone reached the centre of specimens and crystallisation completed (c).

### **3.2.4 Summary of acetone exposure duration**

In summary, immediate characterisation (short-term effects) after direct application of acetone to two distinct polymers showed considerable changes of their mechanical and geometrical properties. The plasticising effect of acetone resulted in significant improvement in strain-at-fracture (up to twenty-five-fold) and toughness (up to three-fold) even for the brittle polymer, PLA. The strength compared to the untreated specimens reduced by 29-87% for PLA and by 37-83% for ABS as immersion time was varied. By demonstrating a multi-fold change in properties, a new capability to integrate this method by hybridisation with the AM process could have significant applications. However, a lack of awareness with respect to the long-term effects of acetone treatment of polymers is evident as no studies investigating this matter for AM parts were found in the literature. Based on the results obtained for the short-term effects, the 10 s immersion time was selected as a reference for a study of the long-term effects of acetone treatment in the next section, since this time provided a balance of brittle and ductile properties.

### **3.3 Long-term effects of acetone**

#### **3.3.1 Mechanical properties**

To study long-term effects, the chemically treated specimens were stored in lab conditions for varying durations - between 1 hour to 60 days - to track recovery of properties. The stress-strain curves along with side-view micrographs of PLA and ABS during their recovery are shown in Figure 8. A distinct difference in terms of rate of recovery between the two polymers is evident. Based on micrographs, ABS recovered rapidly as demonstrated by a flat fracture surface for specimens after 1 hour recovery (Figure 8). Meanwhile, PLA showed considerable ductility and necking (shown by the arrows in Figure 8) and recovered at a slower rate than ABS. For example, after 1 hour of recovery, the strength of PLA specimens was 38.2% lower than specimens tested immediately after chemical treatment, whereas the strength of ABS increased by 31.6% after 1 hour. The ductility for PLA continued to increase twelve-fold up to 10 days, and the yield point was no longer visible. Interestingly, there was a simultaneous increase in strength during this recovery period. The material properties for PLA after 10 days of recovery may be far superior to untreated PLA for some applications since the drastic increase in ductility may justify the approximate 50% reduction in strength. Even with 50% strength loss, PLA still has similar strength to ABS. The ABS recovered 90.5% of its original stress level after 10 days. It took approximately 60 days of recovery for PLA to demonstrate brittle fracture similar to untreated PLA, with 97.2% recovery of initial strength. Interestingly, an improvement in maximum tensile load compared to the untreated specimens of 3.67% was observed after 60 days of recovery: even though strength was slightly lower than the untreated

specimens, redistribution of material into the grooves between layers resulted a better load-bearing structural geometry (by widening the narrowest load bearing area). Such results have never been previously documented for polymers, and this new understanding highlights the potential for new opportunities and applications, including a new design prospects for 4D printing, new methods to reduce mechanical anisotropy, and new hybrid AM-chemical treatment processes to enable tailored control of mechanical properties over predictable timescales.

The obtained stress-strain curves were used to calculate the mechanical properties including strength, tensile modulus and toughness (Figure 9). These properties were normalised by respective values for the untreated specimens. Strain-at-fracture data are discussed with relation to the fracture analysis.

Strength and modulus values for ABS demonstrated more linear trends for a logarithmic timescales and quicker recovery than PLA, for which recovery accelerated after 5 days. The toughness data was slightly scattered for ABS since its values relied on both stress and strain levels. The toughness capability of PLA was considerably improved - twelve-fold after 10 days, which resulted in levels greater than those typically reported in the literature for bulk PLA (e.g. [20,36]); this is discussed in Section 3.3.2 with respect to changes in its thermal properties.

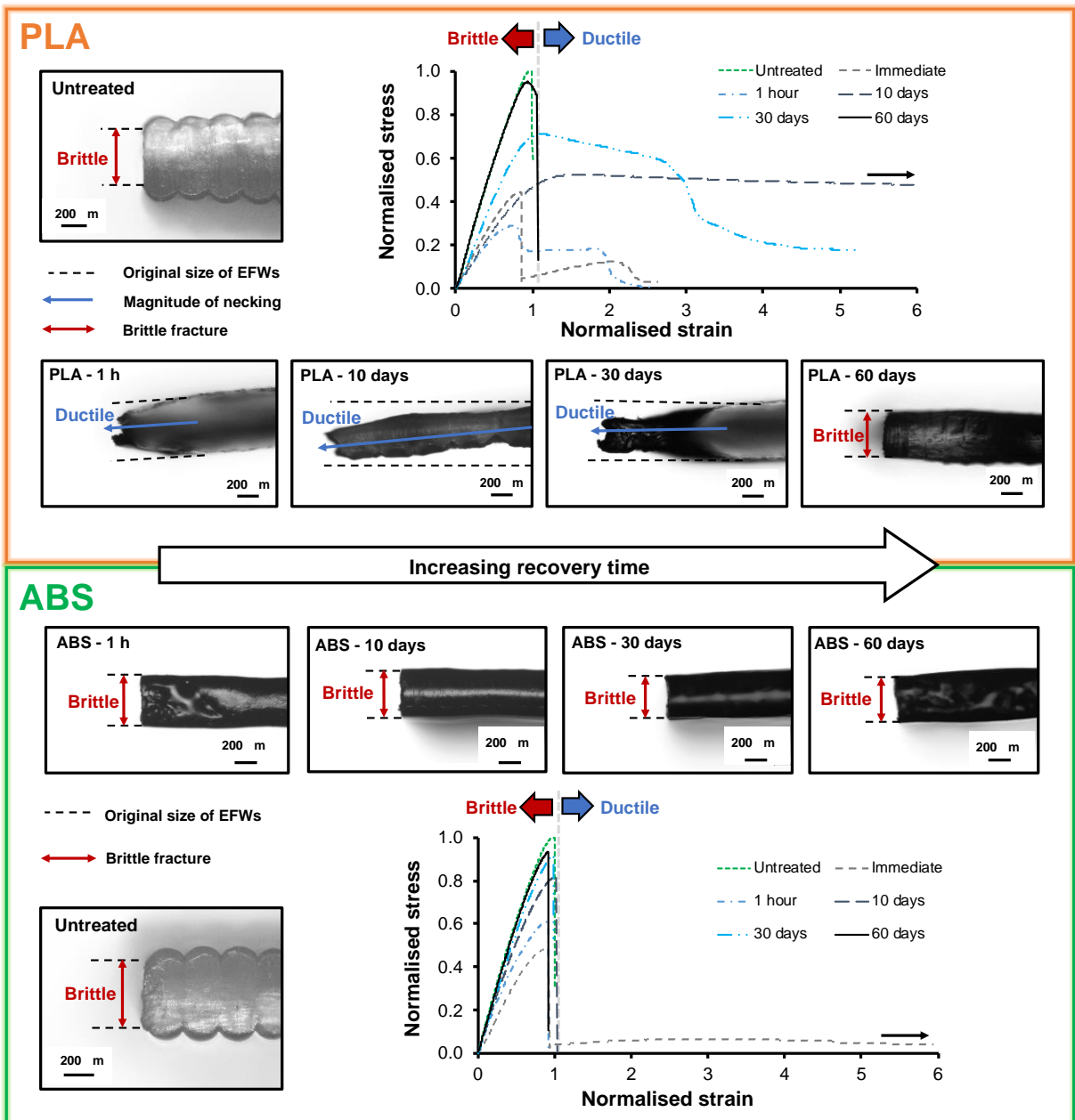


**Figure 8** Stress-strain curves for PLA (top row) and ABS (bottom row) after immersion in acetone for 10 s for various recovery times. PLA showed a slower recovery (50 days more than ABS) to its original state. The side-view images showed the nature of fracture during recovery period. PLA was initially brittle (untreated), changing to ductile-brittle (1 h, 10 days, 30 days) fracture up to 30 days and returning to brittle fracture (60 days). At the same time, ABS showed brittle fracture throughout the entire recovery time.

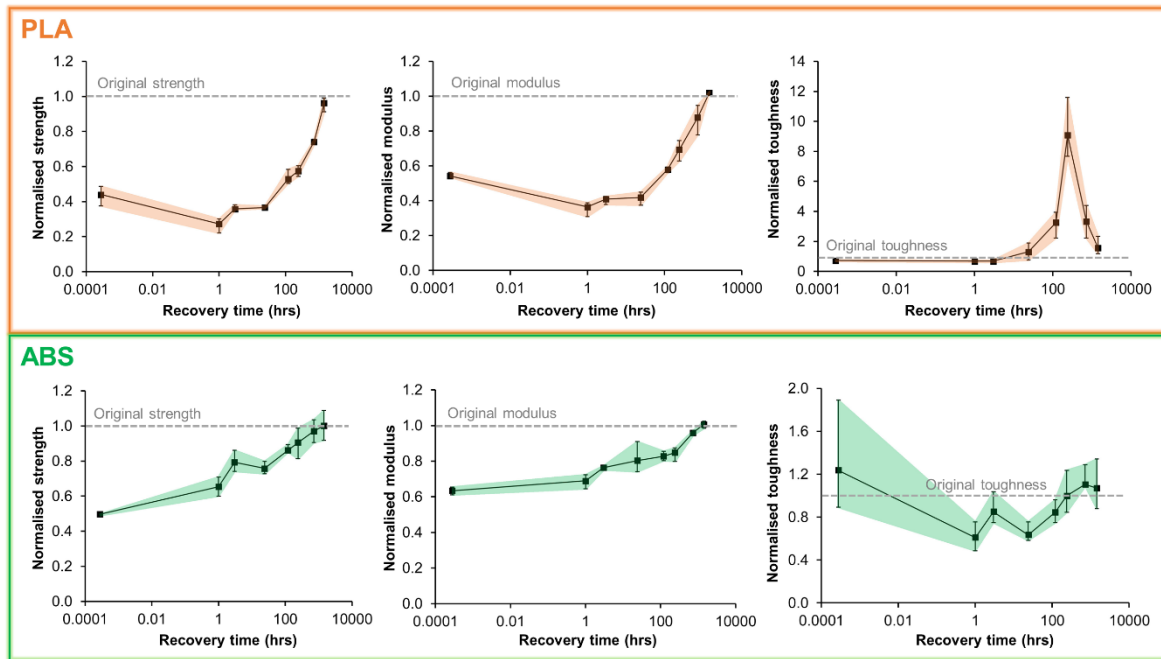


**Figure 9** Evolution of normalised UTS, tensile modulus and toughness for 10 s immersion recovered from 1 hour to 60 days for PLA (top row) and ABS (bottom row). ABS recovered much quicker than PLA. Shaded regions represent the range of data from four replicates.

The relationship between the strain-at-fracture and the brittle-ductile ratio, as investigated for different immersion times in Figure 6, was examined for long-term recovery, and a difference between the two polymers was observed again (Figure 10). PLA micrographs indicated a reduction in the brittle-ductile ratio as plasticity increased until the 10-day measurement when no brittle area was observed. The 10-day recovery also demonstrated the largest deformation for PLA in this study (29.1% compared to 2.95% for untreated). Such results suggested that acetone remained within the polymer structure, continuing to interact with it, and changing its thermal properties. Beyond 10 days, PLA started a transition from a ductile to brittle material with strain-at-fracture capability comparable to that of the untreated specimens after 60 days recovery (2.95% for untreated vs. 4.03% for 60-day recovery). A different trend was observed for ABS, which had a recovery of strain-at-fracture capabilities to that of its original state (i.e. untreated polymer) after just 1 hour. Its brittle-ductile ratio also showed a recovery, further evidencing the higher recovery rate of ABS than PLA.

A narrow range of data for all properties gives confidence that the chemical treatment had a consistent and predictable influence on the materials' properties. Furthermore, the consistency and predictability make it possible to control the mechanical properties and, thus, tailor the recovery to achieve specific and desired outcomes. Thus, the new understanding not only provides a significant new knowledge but can also inform and lead to innovation in

tailoring mechanical properties across different timescales, which could have significant implications to design, manufacturing and postprocessing with MEAM

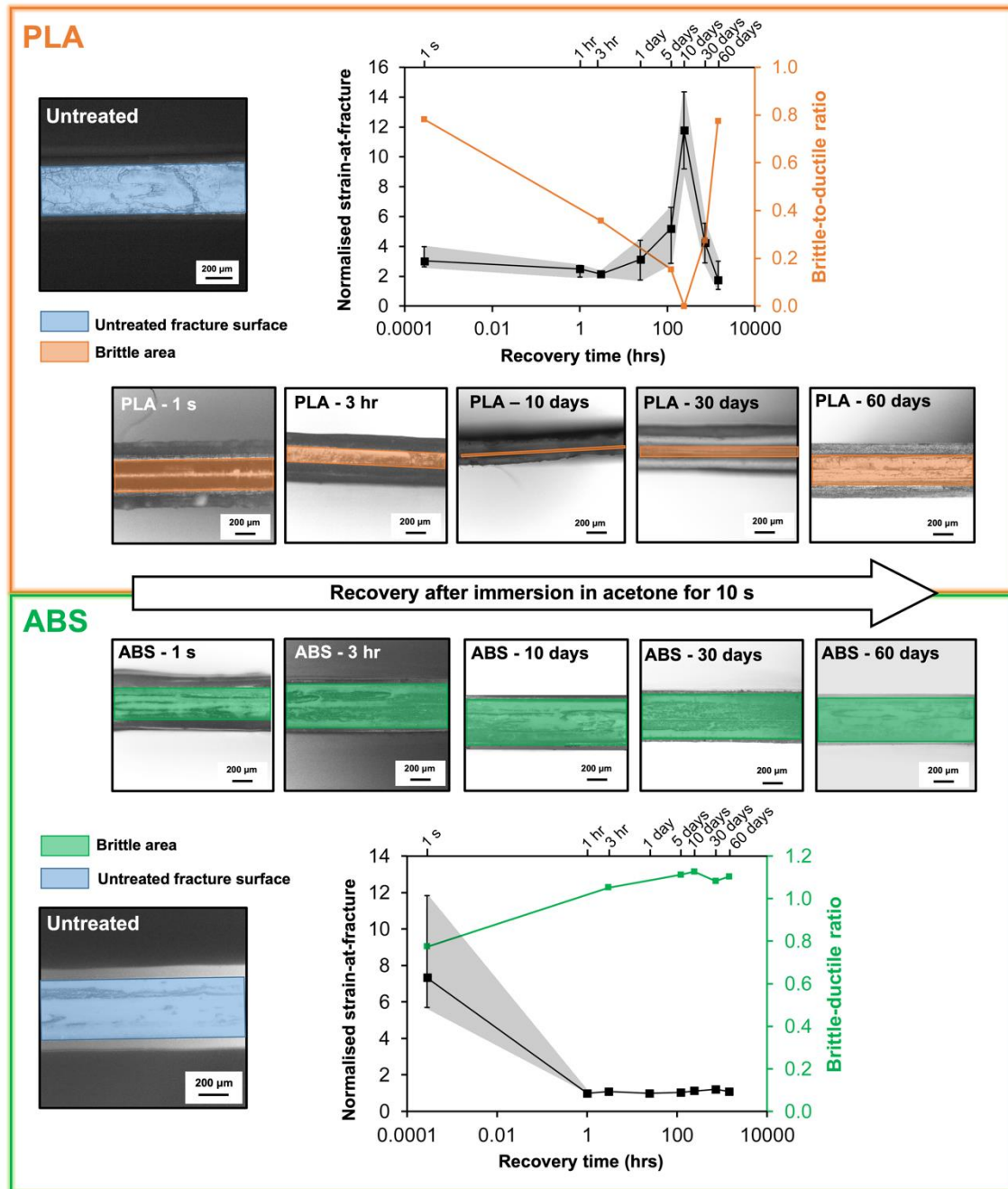


**Figure 10** Fracture surfaces of tested specimens for PLA (top row) and ABS (bottom row) exposed to acetone for 10 s and dried for various times. The graphs show the effect of immersion time on strain-at-fracture and brittle-ductile-ratio.

### 3.3.2 Thermal properties

Thermal properties of PLA at different stages of recovery were measured and presented in Figure 11. As anticipated,  $T_g$  remained unchanged up to 5 days, and was not detected for 10 to 30 days, confirming that the plasticising effect of acetone continued up to 30 days. A slight change in crystallinity was found from 19.1% to 27.9% for immediate (short-term) and 30-day recovery, respectively, as acetone was previously shown (Figure 7) to have a dual effect by inducing both plasticisation and crystallisation of amorphous PLA [34]. Interestingly,  $T_g$  re-appeared after 60 days of recovery at 40.5°C with a slight reduction in crystallinity to 23.1%. Such a trend could be explained by the long-term evaporation of the acetone, which decreased the content of acetone in the crystallised PLA specimens. This in turn resulted in a decrease in the free volume of the amorphous phase of PLA and hence, the  $T_g$  re-appeared. The obtained DSC thermograms agreed with previous study by Naga et al. [34] who studied the effect of acetone immersion on PLA sheets. Such trends complemented the mechanical data, which showed the largest deformation after 10 days of recovery, with the polymer then transitioning back to its untreated properties at 60 days.

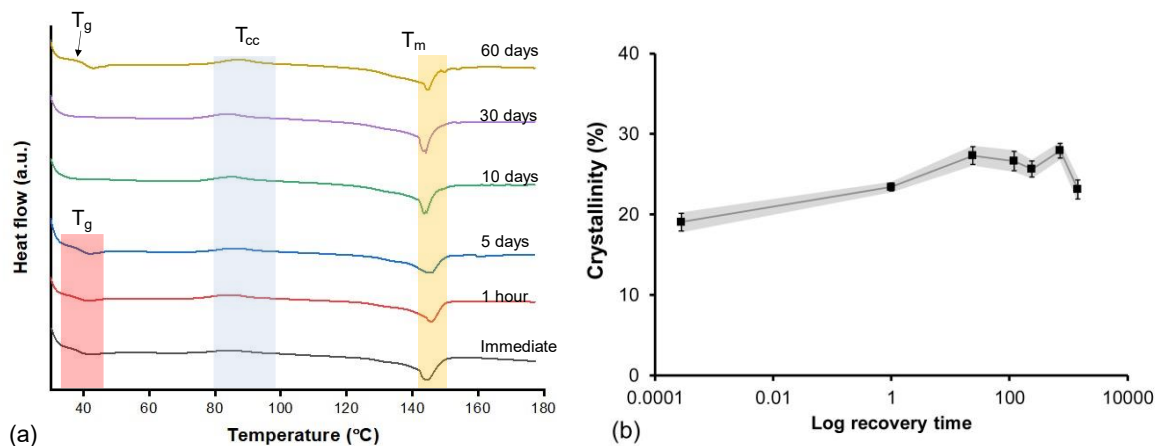


**Figure 11** (a) DSC curves for PLA after exposure to acetone for 10 s and dried for various times.  $T_g$  remained unchanged until 5 days: after that there was no trace of  $T_g$  up to 60 days. (b) Evolution of crystallinity during recovery time showed a slight increase up to 30 days.

### 3.4 Application of results

Significant new understanding of the chemical treatment effects on mechanical properties of ABS and PLA by direct application of acetone was generated. This was the first study to consider the short- and long-term effects of acetone exposure. Repeatable and consistent changes in mechanical and geometrical properties highlight the predictability of results and the potential to support applications in MEAM. This capability to control and adapt mechanical properties for a specific timescale has significant implications for the manufacture of mechanical components by enabling new ways to adapt strength, ductility and toughness

temporarily by selectively modifying the exposure and drying times. For example, for an application where increased stretchability is required for a given time but where the subsequent material strength is required, the use of a selective chemical treatment could provide the required temporary properties. In PLA, this could have major implication for the manufacture of medical devices and patient-specific implants, where not only structural tailoring to the specific recipient is feasible, but also the mechanical properties of specific features, such as hinges, bolt holes or implants could be selectively and controllably modified to meet adaptable demands during implantation. Furthermore, since the obtained results showed evolution of mechanical properties in the long term, such applications could be further extended by taking advantage of this period of evolution. This opens up new avenues for design and implementation of MEAM generated ABS and PLA parts with chemical treatment hybridisation.

It was recognised that, for certain applications, the gradual recovery in PLA is beneficial, while others may require an accelerated recovery similar to that observed in ABS. To address this and further extend the applicability of the chemical treatment method, two types of annealing method (at 80°C) were used and their effect on mechanical performance of PLA was analysed: *pre-annealed* specimens (annealed for 20 days) were treated prior to immersion in acetone for 10 s while *post-annealed* were annealed for 24 hrs after immersion for 10 s. Specimens pre-annealed for 2 hrs recovered mechanical properties faster than untreated specimens (Figure 12). Crystallinity increased eight-fold in 20 days for pre-annealed specimens compared to the untreated specimens. Post-annealed specimens fully recovered properties of the untreated specimens (even marginally exceeding them) with a ten-fold increase in crystallinity within 24 hrs of annealing compared to the untreated specimens. This meant a significant increase in the recovery rate of three- and sixty-fold, respectively. An increase in the strength of 27.8% compared to untreated specimens was observed in the post-annealed specimen after 24 hrs. This indicated an improvement in material distribution for the Z-direction load-bearing capacity compared to that of the printed and untreated specimens. In addition to geometric improvements, annealing may have improved the material properties. These results and methods give an insight into the benefits of annealing the immersed specimens. Direct application of acetone enabled a controlled exposure at constant concentration meaning selective targeting of specific features of material through local application of chemical is possible. This means that specific features or regions could be subjected to mechanical and geometrical changes while retaining untreated properties in others. The method can also be used to generate graded structures within a part without the need to employ two or more materials. Obviously, such treatments are not feasible with the vapour-based method as vaporised chemical cannot be selectively applied.

The applicability of the new understanding was used to develop a new hybrid manufacturing process by combining direct application of acetone and MEAM. This is presented in the next section.

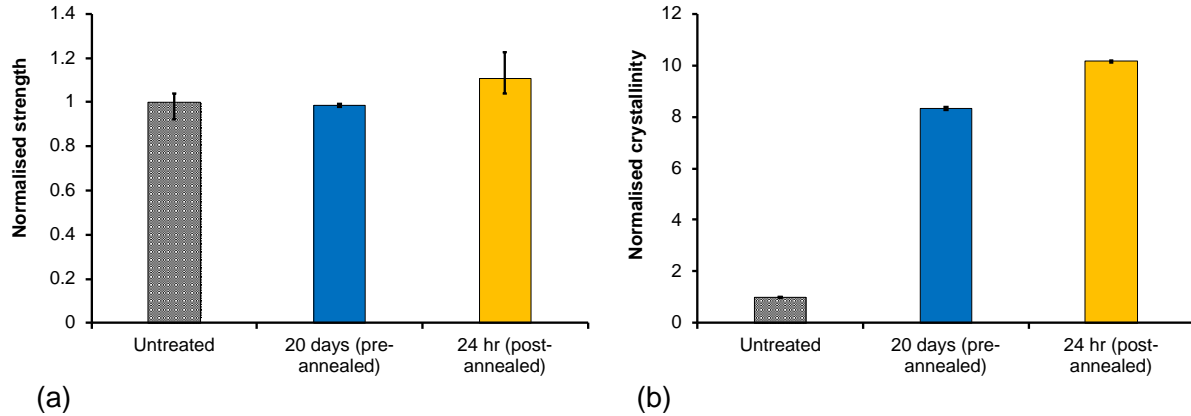


**Figure 12** Normalised strength (a) and crystallinity (b) for different types of PLA specimens (i) untreated; (ii) pre-annealed for 2 hours before chemical treatment and tested after 20 days, and (iii) specimens chemically treated first and then annealed for 24 hours (c).

#### 4 MaTrEx AM - hybrid manufacturing process

Based on the understanding developed in the previous sections, a new hybrid manufacturing process, MaTrEx AM, was developed. This method enabled the material properties achieved by chemical treatment in this study to be utilised in a practical sense. For this purpose, a E3D motion system and tool changer (Figure 13) was used. As demonstrated in Figure 13, the components of this system include the print platform, tool collector, docking station, brush tool, printhead tool and chemical treatment reservoir.

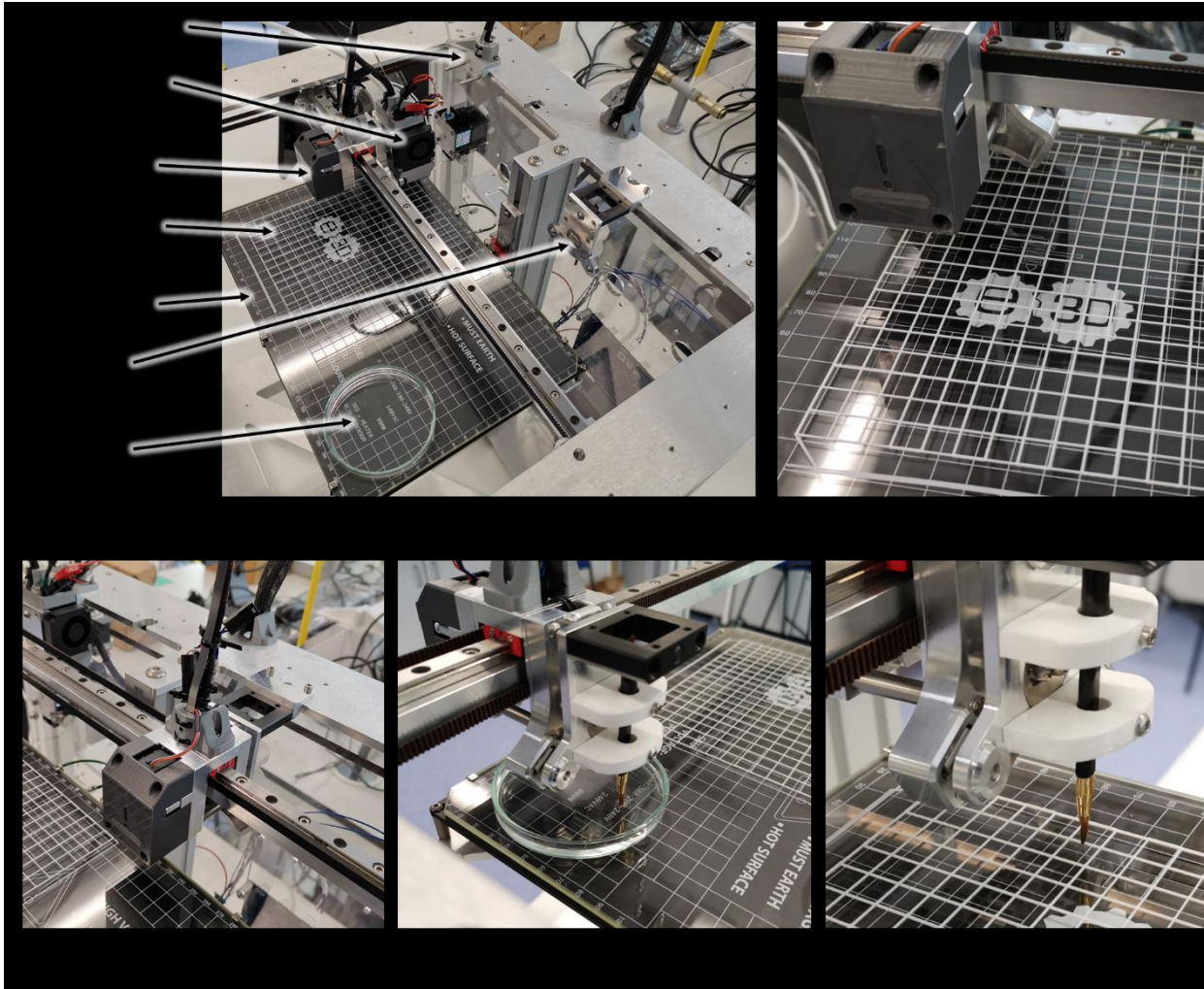


**Figure 13** E3D motion system and tool changer 3D printer used to demonstrate the new hybrid process (MaTrEx AM). (a) Image of the 3D printer highlighting the key features of the system. (b) The printed mesh material (c) The tool collector collects the brush tool. (d) The brush tool is dipped into the chemical treatment reservoir and (e) directly applies the acetone onto specific locations of the mesh material.

#### 4.1 Case study

Based on the knowledge of the material properties of PLA (i.e. low toughness), a case study was devised to validate the potential of MaTrEx AM by selective modification of mechanical properties to increase toughness and govern localised deformation in a relatively brittle mesh material. By explicit design of the GCode with FullControl GCode Designer [37] all manufacturing steps, including printing movements, tool changing, and chemical treatment movements can be created as a single manufacturing procedure. The mesh material was printed as a grid of single extruded filaments (0.5 mm wide and with 9 mm spacing). Six identical mesh materials were printed to achieve three different specimen types (n=2 for each). For selectively chemical treatment, the brush was dipped into the acetone prior to the direct application of the chemical to specific regions in droplet form. After application, the acetone was quickly absorbed or evaporated. In total, there were three treatment regimes, with differing

geometrical designs: (a) untreated control; (b) horizontal treatment and (c) hexagonal treatment, as outlined in Figure 14.

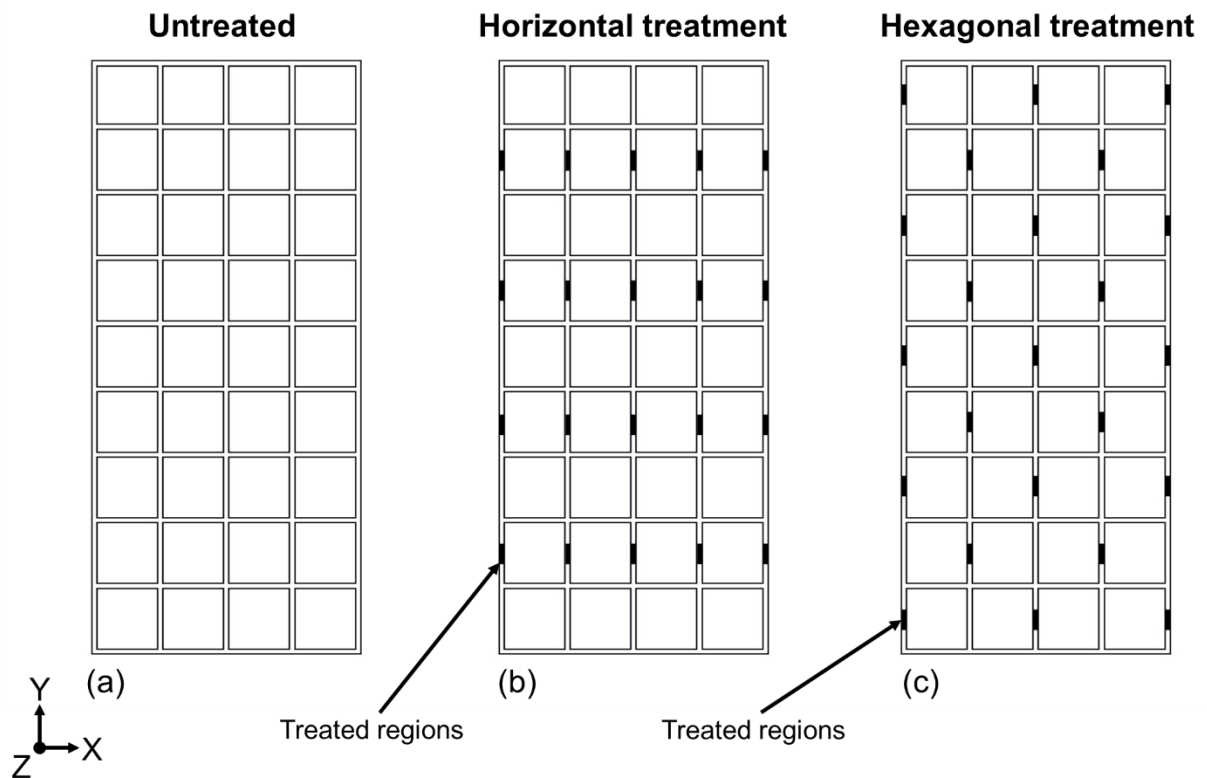


**Figure 14** Schematic of the mesh material for untreated (a), horizontal treatment (b) and hexagonal treatment (c). All mesh materials were identical prior to the selective treatment.

After treatment, mesh materials were mechanically tested using a 1kN load cell at a displacement rate of  $1.5 \text{ mm}\cdot\text{min}^{-1}$  (80 mm gauge distance) and the tensile tests were recorded. The sequence of deformation is shown in Figure 15. At low deformations, all mesh materials were visibly similar (Figure 15 a, c and g). For the control mesh, the material failed abruptly after less than 3.21% strain at the junction where the extruded filaments intersected, as anticipated for a relatively brittle polymer like PLA. However, by selective treatment it was possible to localise deformation in preferred regions depending on the type of the treatment (horizontal and hexagonal). For the horizontal treatment (Figure 15 c-f), direct application of the acetone to the entire row (Figure 14 b) allowed a 27-fold increase in the plastic deformation compared to the untreated specimens. The extensive deformation and yielding of the treated regions is visible in Figure 15 f. The treated regions were elongated and failed after 83.1% strain which is far greater than typical values reported for PLA in the literature. For the hexagonal treatment, the elongation of treated regions allowed a hinge-opening deformation mechanism at intersection points to create a honeycomb-like structure with hexagonal unit cells. For this treatment, the mesh material failed after 43.4% strain, which was lower than the horizontally treated specimen but still an order of magnitude greater than the control. The

### Untreated



(a) 20 s



(b) 60 s

### Horizontal treatment



(c) 20 sec



(d) 400 s



(e) 1000 s



(f) 1600 s

### Hexagonal treatment



(g) 20 sec



(h) 250 s



(i) 500 s



(j) 850 s

**Figure 15** Deformation of mesh material. (a-b) untreated mesh which failed without any significant plastic deformation. (c-f) Horizontal treatment caused deformation to be localised in the treated region and allowed strain of up to 80%. (g-j) Hexagonal treatment was similar to horizontal treatment except the selective treatment led to a hexagonal structure after deformation.

MaTrEx AM process has significant potential for innovative design and material development with MEAM. Application by this process results in selective localised material properties. The earlier part of this study demonstrated how the material properties can be repeatably and predictively controlled by the degree of exposure to acetone. The advantages of hybridisation versus conventional post processing are that it is automated, ensuring consistency and integration within the existing manufacturing workflow. It can also be applied to internal structures of an additively manufactured part. The wide range of solvents available mean that this hybridisation process is suitable for many or all MEAM polymers.

## **5 Conclusions**

In this study, for the first time the short- and long-term effects of acetone immersion on the two most commonly used MEAM materials - ABS and PLA - were analysed. The results demonstrated the suitability of chemical treatment by immersion of specimens, which enabled predictable evolution of mechanical properties. It also enabled selective and localised control of properties which would not have been possible with conventional vapour-based treatment technique. By selecting the appropriate immersion and drying times, it was possible to achieve short-term ductility several times greater than typical values reported in literature, although this was associated with a trade-off of strength. In the long term (up to 60 days after treatment), the effect of acetone diminished, and this occurred at a much quicker rate for ABS than PLA. To demonstrate practical applicability of using acetone to control mechanical properties, a novel hybrid manufacturing process, MaTrEx AM, was developed, which enabled integration of selective chemical treatment into the MEAM workflow. The new understanding and the MaTrEx AM process have significant implications for a range of applications as the desired mechanical properties - strength, strain-at-fracture and toughness - can be attained and controlled by selectively modifying the exposure and drying times.

## **Acknowledgments**

This research did not receive any specific grant from funding agencies in the public, commercial, or not-for-profit sectors.

## Supplementary information

Initially, a vapour treatment with acetone was considered as a known viable post-processing solution, employed particularly for aesthetic purposes with ABS parts [23]. The initial aim was to improve the understanding of mechanical effects of chemical treatment, in addition to aesthetic improvements. An air-tight container was used with an aluminium foil raft to hold the specimens and prevent contact with acetone directly; underneath this, 30 ml of acetone was soaked into paper towelling placed below the aluminium raft. ABS and PLA specimen boxes were sealed in the container and treated for 5 mins, 50 mins and 500 mins.

While the treatment was shown to have a significant impact both geometrically (Figure S1) and mechanically on ABS, and there was some indication of mechanical effect on PLA, a number of limitations of the process were identified:

- ◁ The consistency in concentration of exposure over time and the volume loss for acetone were largely unknown and complex to control.
- ◁ Without such control, an understanding of chemical treatment was limited to qualitative assessment, rather than quantitative measurements.
- ◁ The exposure to acetone could not be targeted to specific regions of the specimen geometry but affected all areas exposed to the vapour.
- ◁ Pooling of liquid acetone at the base of ABS specimens was observed as a consequence of condensation, resulting in damage and its possible variation in concentration of acetone at the base of the specimen.

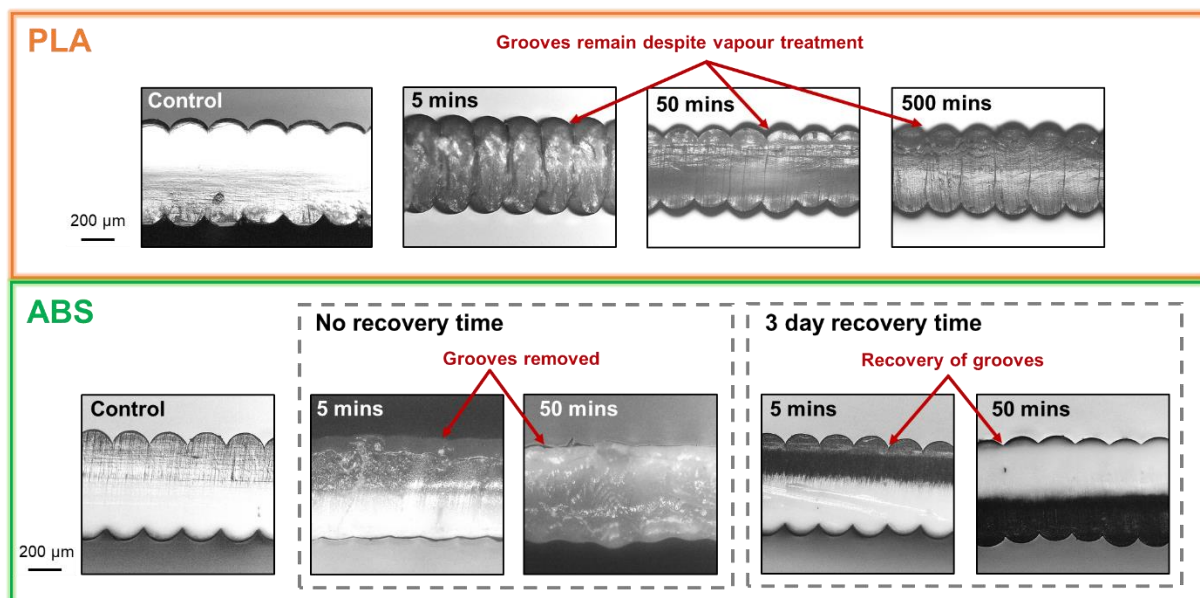


**Figure S1** Sideview micrographs of PLA (top row) and ABS (bottom row) after vapour smooths for 5, 50 and 500 mins. Vapour smoothing appeared to have a very limited immediate effect on geometry of PLA, although it significantly smoothed the grooves for ABS (they were recovered after 3 days of drying).

Given that there were positive indications microscopically and mechanically during this preliminary testing of vapour treatment, a new approach was sought to overcome its limitations.

The method of direct application of acetone via immersion directly addressed the limitations of vapour smoothing, by:

- ◁ Ensuring the consistent concentration of acetone used for immersion during specimen exposure.
- ◁ Enabling controlled exposure times at known treatment concentrations.
- ◁ Possibility to target the desired treatment areas with selective exposure to the liquid.
- ◁ Lack of issues with condensation as the specimen was fully exposed via immersion in liquid.

## References

- [1] P. Honigmann, N. Sharma, B. Okolo, U. Popp, B. Msallem, F.M. Thieringer, Patient-specific surgical implants made of 3D printed PEEK: Material, technology, and scope of surgical application, *Biomed Res. Int.* 2018 (2018) 1–8.  
<https://doi.org/10.1155/2018/4520636>.
- [2] K.C. Wong, 3D-printed patient-specific applications in orthopedics, *Orthop. Res. Rev.* Volume 8 (2016) 57–66. <https://doi.org/10.2147/ORR.S99614>.
- [3] I.S. Pascariu, S.M. Zaharia, Design and Testing of an Unmanned Aerial Vehicle Manufactured by Fused Deposition Modeling, *J. Aerosp. Eng.* 33 (2020) 06020002.  
[https://doi.org/10.1061/\(asce\)as.1943-5525.0001154](https://doi.org/10.1061/(asce)as.1943-5525.0001154).
- [4] S. Ravindrababu, Y. Govdeli, Z.W. Wong, E. Kayacan, Evaluation of the influence of build and print orientations of unmanned aerial vehicle parts fabricated using fused deposition modeling process, *J. Manuf. Process.* 34 (2018) 659–666.  
<https://doi.org/10.1016/j.jmapro.2018.07.007>.
- [5] S. Ahn, M. Montero, D. Odell, S. Roundy, P.K. Wright, Anisotropic material properties of fused deposition modeling ABS, *Rapid Prototyp. J.* 8 (2002) 248–257.  
<https://doi.org/10.1108/13552540210441166>.
- [6] O. Es-Said, J. Foyos, R. Noorani, M. Mendelson, R. Marloth, B. Pregger, Effect of layer orientation on mechanical properties of rapid prototyped samples, *Mater. Manuf. Process.* 15 (2000) 107–122.
- [7] A.K. Sood, R.K. Ohdar, S.S. Mahapatra, Improving dimensional accuracy of Fused Deposition Modelling processed part using grey Taguchi method, *Mater. Des.* 30

- (2009) 4243–4252. <https://doi.org/10.1016/j.matdes.2009.04.030>.
- [8] J.P. Thomas, J.F. Rodríguez, J.E. Renaud, Mechanical behavior of acrylonitrile butadiene styrene (ABS) fused deposition materials. Experimental investigation, *Rapid Prototyp. J.* 7 (2001) 148–158. <https://doi.org/10.1108/13552540110395547>.
- [9] V.E. Kuznetsov, A.N. Solonin, O.D. Urzhumtsev, R. Schilling, A.G. Tavitov, Strength of PLA components fabricated with fused deposition technology using a desktop 3D printer as a function of geometrical parameters of the process, *Polymers (Basel)*. 10 (2018).
- [10] K.G.J. Christiyana, U. Chandrasekhar, K. Venkateswarlu, A study on the influence of process parameters on the mechanical properties of 3D printed ABS composite, *IOP Conf. Ser. Mater. Sci. Eng.* 114 (2016) 012109. <https://doi.org/10.1088/1757-899X/114/1/012109>.
- [11] A. Bellini, S. Gucerì, Mechanical characterization of parts fabricated using fused deposition modeling, *Rapid Prototyp. J.* 9 (2003) 252–264.
- [12] J. Cantrell, S. Rohde, D. Damiani, R. Gurnani, L. Di Sandro, J. Anton, A. Young, A. Jerez, D. Steinbach, C. Kroese, P. Ifju, Experimental characterization of the mechanical properties of 3D printed ABS and polycarbonate parts, *Conf. Proc. Soc. Exp. Mech. Ser. 3* (2017) 89–105. [https://doi.org/10.1007/978-3-319-41600-7\\_11](https://doi.org/10.1007/978-3-319-41600-7_11).
- [13] M. Faes, E. Ferraris, D. Moens, Influence of inter-layer cooling time on the quasi-static properties of ABS components produced via fused deposition modelling, *Procedia CIRP*. 42 (2016) 748–753. <https://doi.org/10.1016/j.procir.2016.02.313>.
- [14] J. Torres, M. Cole, A. Owji, Z. DeMastry, A.P. Gordon, An approach for mechanical property optimization of fused deposition modeling with polylactic acid via design of experiments, *Rapid Prototyp. J.* 22 (2016) 387–404. <https://doi.org/10.1108/RPJ-07-2014-0083>.
- [15] J.A. Travieso-Rodríguez, R. Jerez-Mesa, J. Llumà, O. Traver-Ramos, G. Gomez-Gras, J.J.R. Rovira, Mechanical properties of 3D-printing polylactic acid parts subjected to bending stress and fatigue testing, *Materials (Basel)*. 12 (2019). <https://doi.org/10.3390/ma122333859>.
- [16] M.S. Uddin, M.F.R. Sidek, M.A. Faizal, R. Ghomashchi, A. Pramanik, Evaluating Mechanical Properties and Failure Mechanisms of Fused Deposition Modeling Acrylonitrile Butadiene Styrene Parts, *J. Manuf. Sci. Eng. Trans. ASME*. 139 (2017) 1–12. <https://doi.org/10.1115/1.4036713>.
- [17] T.J. Coogan, D.O. Kazmer, Bond and part strength in fused deposition modeling, *Rapid Prototyp. J.* 23 (2017) 414–422. <https://doi.org/10.1108/RPJ-03-2016-0050>.
- [18] S. Ziemian, M. Okwara, C.W. Ziemian, Tensile and fatigue behavior of layered acrylonitrile butadiene styrene, *Rapid Prototyp. J.* 21 (2015) 270–278.

- <https://doi.org/10.1108/RPJ-09-2013-0086>.
- [19] A. Moetazedian, A. Gleadall, X. Han, V.V. Silberschmidt, Effect of environment on mechanical properties of 3D printed polylactide for biomedical applications, *J. Mech. Behav. Biomed. Mater.* 102 (2020) 103510.  
<https://doi.org/https://doi.org/10.1016/j.jmbbm.2019.103510>.
- [20] J. Allum, A. Moetazedian, A. Gleadall, V. V. Silberschmidt, Interlayer bonding has bulk-material strength in extrusion additive manufacturing: New understanding of anisotropy, *Addit. Manuf.* 34 (2020) 101297.
- [21] J. Allum, A. Gleadall, V. V. Silberschmidt, Fracture of 3D-printed polymers: Crucial role of filament-scale geometric features, *Eng. Fract. Mech.* 224 (2020) 106818.
- [22] A. Moetazedian, A.S. Budisuharto, V. V. Silberschmidt, A. Gleadall, CONVEX (CONTinuously Varied EXtrusion): a new scale of design for additive manufacturing, *Addit. Manuf.* 37 (2021) 101576. <https://doi.org/10.1016/j.addma.2020.101576>.
- [23] H. Gao, D. V. Kaweesa, J. Moore, N.A. Meisel, Investigating the Impact of Acetone Vapor Smoothing on the Strength and Elongation of Printed ABS Parts, *Jom.* 69 (2017) 580–585. <https://doi.org/10.1007/s11837-016-2214-5>.
- [24] P. Wjesundera, J. Schutte, J. Potgieter, The effects of acetone vapour inter-layer processing on fused deposition modelling 3D printed acrylonitrile butadiene styrene, in: *24th Int. Conf. Mechatronics Mach. Vis. Pract.*, 2017: pp. 1–8.  
<https://doi.org/10.1109/M2VIP.2017.8211520>.
- [25] C. Neff, M. Trapuzzano, N.B. Crane, Impact of vapor polishing on surface quality and mechanical properties of extruded ABS, *Rapid Prototyp. J.* 24 (2018) 501–508.  
<https://doi.org/10.1108/RPJ-03-2017-0039>.
- [26] A. Garg, A. Bhattacharya, A. Batish, Chemical vapor treatment of ABS parts built by FDM: Analysis of surface finish and mechanical strength, *Int. J. Adv. Manuf. Technol.* 89 (2017) 2175–2191. <https://doi.org/10.1007/s00170-016-9257-1>.
- [27] S.U. Zhang, J. Han, H.W. Kang, Temperature-dependent mechanical properties of ABS parts fabricated by fused deposition modeling and vapor smoothing, *Int. J. Precis. Eng. Manuf.* 18 (2017) 763–769. <https://doi.org/10.1007/s12541-017-0091-7>.
- [28] A.P. Valerga, S.R. Fernandez-Vidal, F. Girot, A.J. Gamez, On the relationship between mechanical properties and crystallisation of chemically post-processed additive manufactured polylactic acid pieces, *Polymers (Basel)*. 12 (2020) 1–10.  
<https://doi.org/10.3390/POLYM12040941>.
- [29] A.P. Valerga, M. Batista, S.R. Fernandez-Vidal, A.J. Gamez, Impact of chemical post-processing in fused deposition modelling (FDM) on polylactic acid (PLA) surface quality and structure, *Polymers (Basel)*. 11 (2019).  
<https://doi.org/10.3390/polym11030566>.

- [30] A.P. Valerga Puerta, S.R. Fernandez-Vidal, M. Batista, F. Girot, Fused deposition modelling interfacial and interlayer bonding in PLA post-processed parts, *Rapid Prototyp. J.* 26 (2019) 585–592. <https://doi.org/10.1108/RPJ-06-2019-0176>.
- [31] ASTM D1708-18, Standard Test Method for Tensile Properties of Plastics By Use of Microtensile, 2002.
- [32] A. Moetazedian, A. Gleadall, X. Han, A. Ekinci, E. Mele, V.V. Silberschmidt, Mechanical performance of 3D printed polylactide during degradation, *Addit. Manuf.* 38 (2021) 101764. <https://doi.org/https://doi.org/10.1016/j.addma.2020.101764>.
- [33] O. Vyavahare, D. Ng, S.L. Hsu, Analysis of structural rearrangements of poly(lactic acid) in the presence of water, *J. Phys. Chem. B.* 118 (2014) 4185–4193. <https://doi.org/10.1021/jp500219j>.
- [34] N. Naga, Y. Yoshida, M. Inui, K. Noguchi, S. Murase, Crystallization of Amorphous Poly(lactic acid) Induced by Organic Solvents, *J. Appl. Polym. Sci.* 119 (2011) 2058–2064. <https://doi.org/10.1002/app.32890>.
- [35] N. Naga, Y. Yoshida, K. Noguchi, S. Murase, Crystallization of Amorphous Poly(Lactic Acid) Induced by Vapor of Acetone to Form High Crystallinity and Transparency Specimen, *Open J. Polym. Chem.* 3 (2013) 29–33. <https://doi.org/10.4236/ojpchem.2013.32006>.
- [36] S. Farah, D.G. Anderson, R. Langer, Physical and mechanical properties of PLA, and their functions in widespread applications — A comprehensive review, *Adv. Drug Deliv. Rev.* 107 (2016) 367–392.
- [37] A. Gleadall, A. Gleadall, FullControl GCode Designer: open-source software for unconstrained design in additive manufacturing. *Additive Manufacturing* (2021) 102109. Version Heron01. Software available at: [www.fullcontrolgcode.com](http://www.fullcontrolgcode.com), (2020). <http://fullcontrolgcode.com> (accessed February 23, 2020).